



# Precipitation extremes on multiple time scales – Bartlett-Lewis Rectangular Pulse Model and Intensity-Duration-Frequency curves

Christoph Ritschel<sup>1</sup>, Henning W. Rust<sup>1</sup>, and Uwe Ulbrich<sup>1</sup>

<sup>1</sup>Institut für Meteorologie, Freie Universität Berlin, Carl-Heinrich-Becker-Weg 6-10, D-12165  
Berlin, Germany

*Correspondence to:* Christoph Ritschel (christoph.ritschel@met.fu-berlin.de)

**Abstract.** For several hydrological modelling tasks, precipitation time-series with a high (i.e. sub-daily) resolution are indispensable. This data is, however, not always available and thus model simulations are used to compensate. A canonical class of stochastic models for sub-daily precipitation are Poisson-cluster processes, with the Bartlett-Lewis rectangular pulse model (BLRPM) as a prominent  
5 representative. The BLRPM has been shown to well reproduce certain characteristics found in observations. Our focus is on intensity-duration-frequency relationship (IDF), which are of particular interest in risk assessment. Based on a high resolution precipitation time-series (5-min) from Berlin-Dahlem, BLRPM parameters are estimated and IDF curves are obtained on the one hand directly from the observations and on the other hand from BLRPM simulations. Comparing the resulting  
10 IDF curves suggests that the BLRPM is able to reproduce main features of IDF statistics across several durations but cannot capture singular events (here an event of magnitude 5 times larger than the second largest event). Here, IDF curves are estimated based on a parametric model for the duration dependence of the scale parameter in the General Extreme Value distribution; this allows to obtain a consistent set of curves over all durations. We use the BLRPM to investigate the validity of this  
15 approach based on simulated long time series.

## 1 Introduction

Precipitation is one of the most important atmospheric variables. Large variations on spatial and temporal scales are observed, i.e. from localised thunderstorms lasting a few tens of minutes up to mesoscale hurricanes lasting for days. Precipitation on every scale affect everyday life: short but  
20 intense extreme precipitation events challenge the drainage infrastructure in urban areas or might put agricultural yields at risk; long-lasting extremes can lead to flooding (Merz et al., 2014). Both, short intense and long-lasting large-scale rainfall can lead to costly damages, e.g. the floodings in Germany in 2002 and 2013 (Merz et al., 2014), and are therefore subject of research.



Risk quantification is based on an estimated frequency of occurrence for events of a given intensity and duration. This information is typically summarised in an Intensity-Duration-Frequency (IDF) relationship (e.g., Koutsoyiannis et al., 1998), also referred to as IDF curves. These curves are typically estimated from long observed precipitation time-series, mostly with a sub-daily resolution to include also short durations into the IDF relationship. These are indispensable for some hydrological applications, e.g., extreme precipitation characteristics are derived from IDF curves for planning, design and operation of drainage systems, reservoirs and other hydrological structures. One way to obtain IDF curves is modelling block-maxima for fixed duration with the generalised extreme value distribution (GEV, e.g., Coles, 2001). Here, we employ a parametric extension to the GEV which allows a simultaneous modelling of extreme precipitation for all durations Koutsoyiannis et al. (1998); Soltyk et al. (2014).

Due to a limited availability of observed high-resolution records with adequate length, simulations with stochastic precipitation models are used to generate series for subsequent studies (e.g., Khaliq and Cunnane, 1996; Smithers et al., 2002; Vandenberghe et al., 2011). The advantage of stochastic models are their comparably simple formulation and their low computational costs allowing to quickly generate large ensembles of long precipitation time-series. A review of these models is given in, e.g., Onof et al. (2000); Wheater et al. (2005). A canonical class of sub-daily stochastic precipitation models are Poisson cluster models with the Bartlett-Lewis rectangular pulse model (BLRPM) as a prominent representative (Rodriguez-Iturbe et al., 1987, 1988; Onof and Wheater, 1994b; Wheater et al., 2005). The BLRPM has been shown to well reproduce certain characteristics found in precipitation observations (Rodriguez-Iturbe et al., 1987). Due to the high degree of simplification of the precipitation process, the model is known to have difficulties in extremes. Nevertheless, it is still part of a well-established class of precipitation models and thus subject to investigation in this paper.

The BLRPM and intensity-duration-frequency relationships are of particular interest to hydrological modelling and impact assessment. In the following, we address the three research questions by means of a case study: 1) Is the BLRPM able to reproduce the intensity-duration relationship found in observations?, 2) How are IDF curves affected by singular extreme events which might not be reproducible with the BLRPM? and 3) is the parametric extension to the GEV a valid approach to obtain IDF curves? For the class of multi-fractal rainfall models, question 1) has been addressed by Langousis and Veneziano (2007).

Section 2 gives a short overview the BLRPM variant used here, Sect. 3 briefly explains IDF curves and discusses a parametric model to estimate them from precipitation time series. This is followed by a description of the data used (Sect. 4). The results section (Sect.5) starts with a description of the BLRPM parameter estimates for the case study area (Sect. 5.1), investigates the capability of this model to reproduce IDF curves (Sect. 5.2) and discusses the influence of a singular extreme (Sect. 5.3) It closes with a comparison of singular duration GEV quantiles with the duration dependent GEV approach to IDF curves (Sect. 5.4). Section 6 discusses results and concludes the paper.



## 2 Bartlett-Lewis rectangular pulse model

From early radar based observations of precipitation, a hierarchy of spatio-temporal structures was suggested by Pattison (1956) and Austin and Houze (1972): intense rain structures (denoted as cells) tend to form in the vicinity of existing cells and thus cluster in larger structures, so called storms or cell clusters. Occurrence of these cells and storms (cell clusters) can be described using Poisson-processes. This makes the Poisson-cluster process a natural approach to stochastic precipitation modelling.

The idea of modelling rainfall with stochastic models exists since Cam (1961) modelled rain gauge data with a Poisson-cluster process. Later, Waymire et al. (1984) and Rodriguez-Iturbe et al. (1987) continued the development of this type of model. Poisson-cluster rainfall models are characterised by a hierarchy of two layers of Poisson processes.

Similarly to various others studies (e.g., Onof and Wheeler, 1994a; Cowpertwait, 1998; Kaczmarek, 2011), we choose the Bartlett-Lewis rectangular pulse model (BLRPM), a popular representative of Poisson-cluster models with set of five physically interpretable parameters (Rodriguez-Iturbe et al., 1987). At the first level cell clusters (storms) are generated according to a Poisson-process with a cluster generation rate  $\lambda$  and an exponentially distributed life-time with expectation  $1/\gamma$ . Within each cell cluster, cells are generated according to a Poisson process with cell generation rate  $\beta$  and exponentially distributed life-time with expectation  $1/\eta$ , hence the term Poisson-cluster process. Associated with each cell is a precipitation intensity being constant during cell life-time, exponentially distributed with mean  $\mu_x$ . The constant precipitation intensity in one cell gave rise to the name rectangular pulse. Model parameters are summarised in the parameter vector  $\theta = \{\lambda, \gamma, \beta, \eta, \mu_x\}$ . Figure 1 shows a sketch of the BLRPM illustrating the two levels: start of cell-clusters (storms) are shown as red dots, within each clusters, cells (blue rectangular pulses) are generated during the clusters' life-time starting from the cluster origin. The cells' lifetime is shown as horizontal and their precipitation intensity as vertical extension in Fig. 1; cells can overlap. This continuous time model yields a sequence of pulses (cells) with associated intensity, see Fig. 2 (top panel). Adding up the intensity of overlapping pulses yields a time continuous step-function (Fig. 2, middle panel). Although time continuous, this function is not continuously differentiable in time due to the rectangular pulses. Observational time series are typically also not continuously differentiable as they are discretised in time. Summing up the resulting continuous series for discrete time intervals makes it comparable with observations and renders unimportant the artificial jumps from the rectangular pulses present in the continuous series, Fig. 2 (bottom layer).

An alternative to the Bartlett-Lewis process is the Neyman-Scott process (Neyman and Scott, 1952). The latter is motivated from observations of the distribution of galaxies in space. In the Neyman-Scott process cells are distributed around the centre of a cell cluster. Both are prototypical models for sub-daily rainfall and are discussed in more detail in Wheeler et al. (2005).

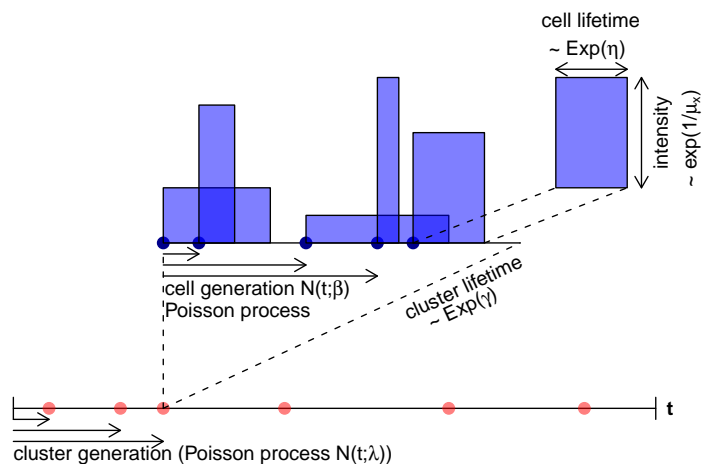


**Figure 1.** Scheme of the Bartlett-Lewis rectangular pulse model. A similar scheme can be found in Wheatler et al. (2005)

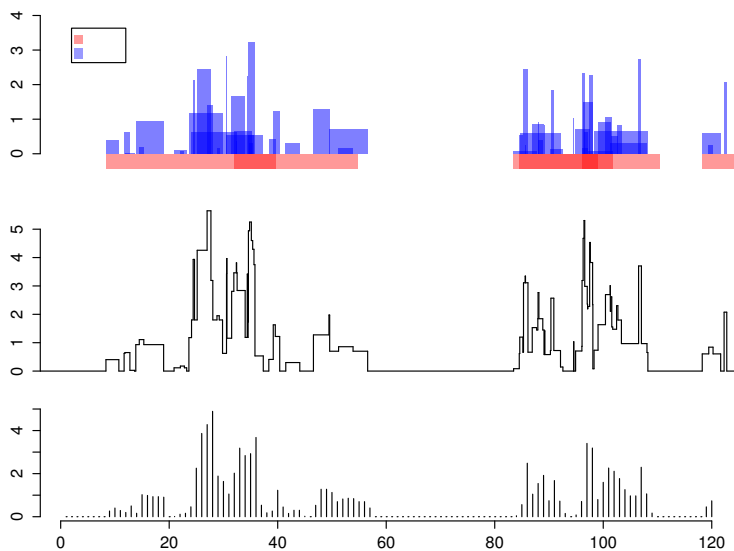


**Figure 2.** Example realisation of the BLRPM. Top layer shows the continuously simulated storms and cells. The plot in the middle layer combines the cell intensities to continuous-time a step function. The bottom layer shows the precipitation series summed up for discrete time intervals. Parameters used for this simulation:  $\lambda = 4/120$ ,  $h^{-1}, \gamma = 1/15$ ,  $h^{-1}, \beta = 0.4$ ,  $h^{-1}, \eta = 0.5$ ,  $h^{-1}, \mu_x = 1\text{mm/h}^{-1}$ .



Several studies (Onof and Wheater, 1994b; Cowpertwait et al., 2007; Kim et al., 2013) already investigated these kind of precipitation models and some applications are known (Cowpertwait et al., 1996a, b; Verhoest et al., 1997).

100 Parameter estimation for the BLRPM is by far not trivial. The canonical approach is a method-of-moment-based estimation (Rodriguez-Iturbe et al., 1987)) using the objective function

$$Z(\boldsymbol{\theta}; \mathbf{T}) = \sum_{i=1}^k w_i \left[ 1 - \frac{\tau_i(\boldsymbol{\theta})}{T_i} \right]^2. \quad (1)$$

This function relates moments  $\tau_i(\boldsymbol{\theta})$  derived from the model with parameters  $\boldsymbol{\theta}$  to empirical moments  $T_i$  from the time series. The set of  $k$  moments  $T_i$  is typically chosen from the first and second  
105 moments obtained for different aggregation times  $h$ . Here, we use the mean, the variances, the lag-1 auto-covariance function and the probability of zero rainfall for  $h \in \{1h, 3h, 12h, 24h\}$ , similar to (Kim et al., 2013), and thus end up with  $k = 13$  moments  $T_i$ . Their analytic counterparts  $\tau_i(\boldsymbol{\theta})$  are derived from the model. The weights in the objective function were chosen to be  $w_{i=1} = 100$  and  $w_{i \neq 1} = 1$ , similar to (Cowpertwait et al., 1996a), emphasising the first moment  $T_1$  (mean) 100 times  
110 more than the other moments.

It turns out that  $Z(\boldsymbol{\theta}; \mathbf{T})$  has multiple local minima. To avoid those, the optimisation is repeated many times with different initial guesses for the parameters. These initial guesses are sampled from a range of feasible values in parameter space in a Latin-Hypercube fashion (McKay et al., 1979). As only positive model parameters are meaningful, optimisation is performed on log-transformed  
115 parameters. Similarly to Cowpertwait et al. (2007), we use a symmetric objective function

$$Z(\boldsymbol{\theta}; \mathbf{T}) = \sum_{i=1}^k w_i \left\{ \left[ 1 - \frac{\tau_i(\boldsymbol{\theta})}{T_i} \right]^2 + \left[ 1 - \frac{T_i}{\tau_i(\boldsymbol{\theta})} \right]^2 \right\}. \quad (2)$$

A few tests indicate that this objective function is robust and faster in convergence (not shown). Numerical optimisation techniques based on gradient calculations, e.g. *Nelder-Mead* (Nelder and Mead, 1965) or *BFGS* (Broyden, 1970; Fletcher, 1970; Goldfarb, 1970; Shanno, 1970), are typically  
120 used. We use R's `optim()` function (R Core Team, 2016) choosing *L-BFGS-B* as the underlying optimisation algorithm R Core Team (2016) allowing to set additional constraints in parameter space. 100 different sets of initial guesses for the parameters sampled in a Latin-Hypercube way are used.

Models of this type suffer from parameter non-identifiability, meaning that qualitatively different sets of parameters lead to minima of the objective function with comparable values (Verhoest et al.,  
125 1997). A more detailed view on global optimisation techniques and comparisons between different objective functions is given in Vanhaute et al. (2012).

The R-package BLRPM provides functions for simulation and parameter estimation and is available from the authors on request.



### 3 Intensity-Duration-Frequency

130 Intensity-duration-frequency (IDF) curves show *return-levels* (intensities) for given *return-periods*  
 (inverse of frequencies) as a function of *rainfall duration*. Their formulation goes back to Bernard  
 (1932). They are frequently used for supporting infrastructure risk assessment (e.g., Simonovic and  
 Peck, 2009; Cheng and AghaKouchak, 2013). IDF curves are an extension to classical extreme value  
 135 statistics. The latter aims at better characterising the tails of a distribution by using parametric models  
 derived from limit theorems (e.g., Embrechts et al., 1997). There are two main approaches: modelling  
 block-maxima (e.g., maxima out of monthly or annual blocks) with the generalised extreme value  
 distribution (GEV) or modelling threshold excesses with the generalised Pareto distribution (GPD)  
 (e.g., Coles, 2001; Embrechts et al., 1997). We choose the block-maxima approach with the general  
 extreme value distribution

$$140 \quad G(z) = \exp \left\{ - \left[ 1 + \xi \left( \frac{z - \mu}{\sigma} \right) \right]^{-\frac{1}{\xi}} \right\} \quad (3)$$

as parametric model for the block-maxima  $z$ . The GEV is characterised by the location parameter  $\mu$ ,  
 the scale parameter  $\sigma$  and the shape parameter  $\xi$ . These can be estimated from block-maxima using  
 a maximum-likelihood estimator (e.g., Coles, 2001). Here, we use maxima from monthly blocks. To  
 avoid mixing maxima from different seasons, a set of GEV parameters is estimated for all maxima  
 145 from January, another set for all maxima from February and so on. For a given month, GEV param-  
 eters are estimated for various durations (or aggregation times), e.g.  $d \in \{1h, 6h, 12h, 24h, 48h, \dots\}$ .  
 An IDF curve for a given return-period  $T = 1/(1-p)^{1/\xi}$  can then be constructed from  $p$ -quantiles  
 $Q_{p,d}$  from GEVs for different durations  $d$  by means of fitting a parametric model (e.g., Koutsoyian-  
 nis et al., 1998). As the estimated IDF-curve  $IDF_{T_1}(d)$  for return-period  $T_1$  is independent of the  
 150 estimate of another curve  $IDF_{T_2}(d)$  with return-period  $T_2 > T_1$ , there is no constraint ensuring  
 $IDF_2(d) > IDF_1(d)$  for arbitrary durations  $d$ . Consequently, this approach easily leads to incon-  
 sistent (i.e. crossing) IDF-curves. For example for a given duration  $d$ , the 50-year return-level can  
 exceed the 100-year return-level.

To overcome these problems and increase robustness in constructing IDF curves, Koutsoyiannis  
 155 et al. (1998) suggested a duration-dependent scale parameter  $\sigma_d$

$$\sigma_d = \frac{\sigma}{(d + \theta)^\eta}, \quad (4)$$

with  $\theta$ ,  $\eta$  and  $\sigma$  being independent of the duration  $d$ . The parameter  $\eta$  quantifies the slope of the IDF  
 curve in the main region and  $\theta$  controls the deviation of the power-law behaviour for short durations.  
 Furthermore, location is re-parametrised by  $\tilde{\mu} = \mu/\sigma_d$  which is now independent of durations  $d$ ,  
 160 such is the shape parameter  $\xi$ . This lead to a parametric formulation of a duration-dependent GEV

<sup>1</sup> $p$  denotes the non-exceedance probability.



distribution

$$F(x; \mu, \sigma_d, \xi) = \exp \left\{ - \left[ 1 + \xi \left( \frac{x}{\sigma_d} - \mu \right) \right]^{\frac{-1}{\xi}} \right\}. \quad (5)$$

This formulation allows consistent modelling of rainfall maxima across different durations  $d$  using a single distribution at the cost of only two additional parameters. These parameters can be analogously estimated by maximum-likelihood (Solyk et al., 2014). To avoid local minima when optimising the likelihood, we repeat the optimisation with different sets of initial guesses for the parameters, sampled according to a Latin-Hypercube scheme analogously to the BLRPM parameter estimation. This method of constructing IDF curves is consistent in the sense that curves for different return-periods cannot cross. We refer to this approach as the *duration-dependent GEV* approach (dd-GEV).

However, the data points for different durations are dependent (as they are derived from the same underlying high-resolution data set by aggregation) and thus the i.i.d. assumptions required for maximum-likelihood estimation is not fulfilled. Consequently, confidence intervals are not readily available from asymptotic theory; they can be estimated by bootstrapping.

## 4 Data

A precipitation time series from the station *Botanical Garden* in Berlin-Dahlem, Berlin, Germany is used as a case study. A tipping-bucket registers precipitation amounts at 1-min resolution. For the analysis at hand, a 13 year time series with 1-min resolution from the years 2001-2013 is available. The series is aggregated to durations  $d \in \{1h, 2h, 3h, 6h, 12h, 24h, 48h, 72h\}$  yielding 8 time series with different temporal resolution. IDF parameters are estimated using annual maxima for each month of the year individually using all 8 duration series..

## 5 Results

### 5.1 Estimation of BLRPM parameters

Minimising the symmetric objective function (Eq. (2)) yields BLRPM parameter estimates individually for every month of the year, shown in Fig. 3 and explicitly given in Tab. 1 in Appendix A. The resulting BLRPM parameters are reasonable compared to observed precipitation characteristics: Large mean intensities  $\hat{\mu}_x$  and short mean cell life-times  $1/\hat{\eta}$  in summer correspond to precipitation being dominated by convective events. Similar, the mean cluster life-time  $1/\hat{\gamma}$  decreases in summer, whereas the mean cell generation rate  $\hat{\beta}$  increases. Vice versa, in winter small intensities and long storm durations correspond to stratiform precipitation patterns, typically dominating the winter precipitation in Germany. The storm generation rate  $\lambda$  show only a minor seasonal variation.

With the BLRPM parameter estimates (Tab. 1, Sect. A) 1000 realisations with the same length as the observations (13 years) are generated. From both, the original precipitation series and the set

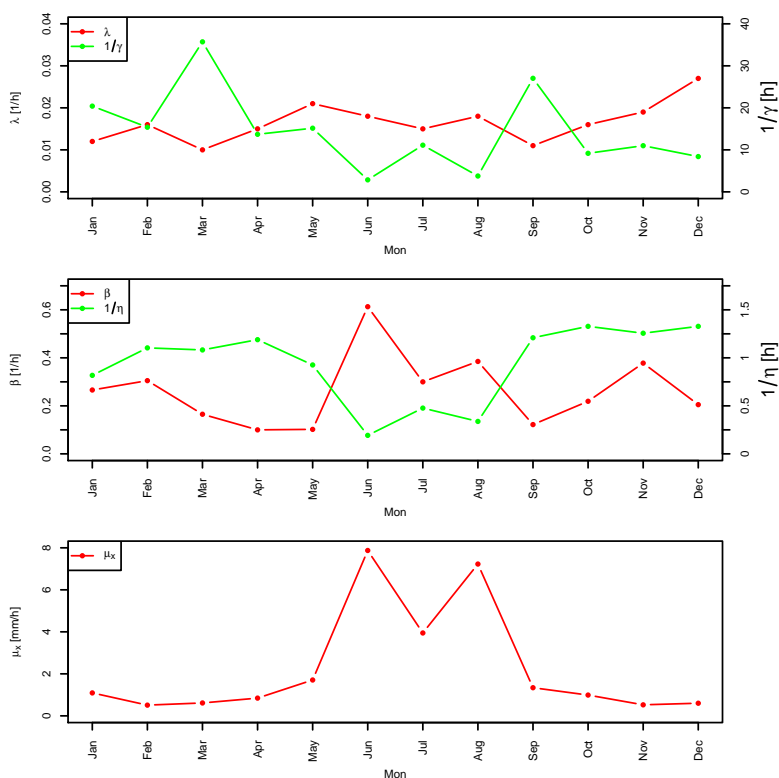


**Figure 3.** BLRPM parameter estimates for all month of the year obtained from the Berlin-Dahlem precipitation time series. Top: cell-cluster generation rate  $\lambda$  and cluster lifetime  $1/\gamma$ ; middle: cell generation rate  $\beta$  and cell lifetime  $1/\eta$ ; bottom: cell mean intensities  $\mu_x$ .

of simulated time series, we derived a set of statistics for model validation. The first moment  $T_1$   
 195 – the mean – is very well represented (not shown) as it enters the objective function with weight  
 $w_1 = 100$  compared to weights of 1 for the other statistics. Figure 4 shows the variance for 6-hourly  
 aggregation and the probability of zero rainfall; for all months the 6h-variances of simulated and  
 observed series are in good agreement. This is particularly noteworthy as the 6-hourly aggregation  
 was not used for parameter estimation. Similar to previous studies (e.g., Onof and Wheater, 1994a),  
 200 the model fails to reproduce the probability of zero rainfall, here exemplary shown for the 12-hourly  
 aggregation. The model mainly overestimates it and therefore has shortcomings in the representation  
 of the time distribution of events (Rodriguez-Iturbe et al., 1987; Onof and Wheater, 1994a).

An important aspect for hydrological applications, is the model's ability to reproduce extremes on  
 various temporal scales. This behaviour is investigated in the next section with the construction of  
 205 IDF curves.



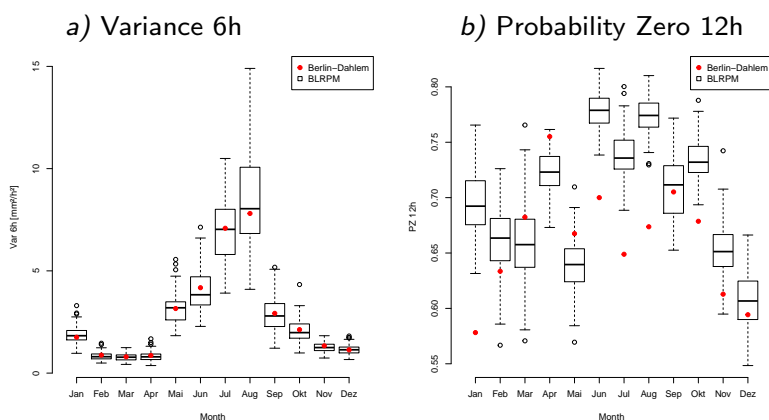


**Figure 4.** Comparison of statistics derived from the observational record (red dots) and 1000 simulated time-series (box plots): a) variance at 6-hourly aggregation level and b) probability of zero rainfall at 12-hourly aggregation.

## 5.2 Intensity-Duration-Frequency curves from BLRPM simulations

Monthly block-maxima for every month in the year are drawn for various durations from the observational time series and 1000 BLRPM simulations of same length, This is the basis for estimating GEV distributions for individual durations, as well as for constructing dd-GEV IDF curves.

210 IDF curves for Berlin-Dahlem obtained from observation are shown as dotted lines in Fig. 5 for January, April, July and October for the 0.5-quantile (2-year return-period, red), 0.9-quantile (10-year return-period, green) and the 0.99-quantile (100-year return-period, blue). Analogously, IDF curves are derived from 1000 simulations of the BLRPM precipitation series, cf. Sect. 5.1. The coloured shading in Fig. 5 give the range of variability (5% to 95%) for these 1000 curves with the median highlighted as dotted line. Except for January, the curves obtained directly from the observational series can be found within the range of variability of curves derived from the BLRPM. The main IDF features from observations are well reproduced by the BLRPM: the power-law-like behaviour (straight line in the double-logarithmic representation) in July extending almost across the full range of durations shown, as well as the flattening of the IDF curves for short durations for April and September. There is, however, a tendency for the BLRPM to underestimate extremes, particularly for large return-levels and long durations, as can be seen from plots of relative differences in IDF curves (Fig. 9) in Appendix B.

220

We interpret the different behaviour for short durations (flattening vs continuation of the straight line) for summer (July) and the remaining seasons as a result of different mechanisms governing extreme precipitation events: while convective events dominate in summer, frontal and thus more large scale events dominate in the other seasons.

225

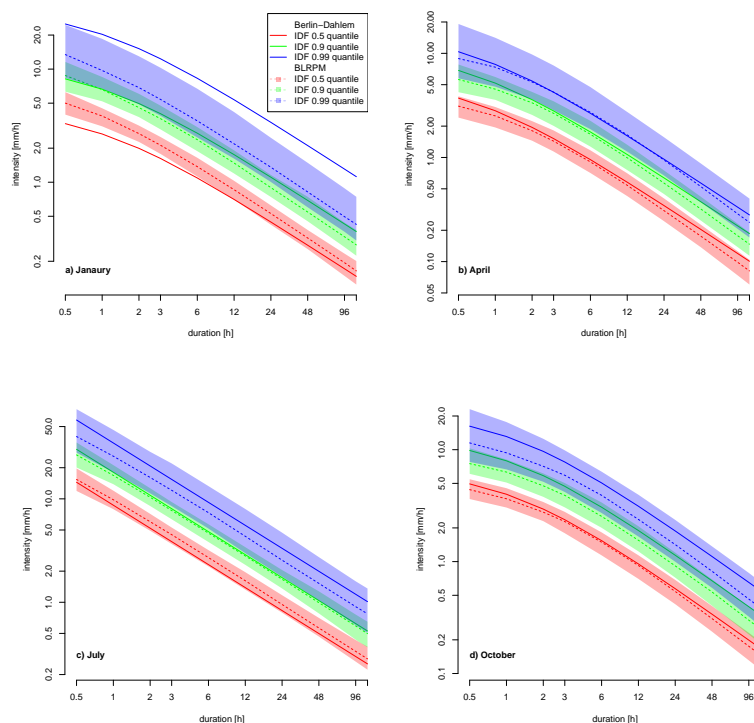


**Figure 5.** IDF curves obtained via dd-GEV for a) January, b) April, c) July and d) October: 0.5 (red), 0.9 (green) and 0.99-quantiles (blue) corresponding to 2-yr, 10-yr, and 100-yr return-periods, respectively. Solid lines are derived directly from the Berlin-Dahlem time series. Coloured shading mark the central 90% range of variability of IDF curves obtained in the same manner with same colour code but from 1000 BLRPM simulations (Sect 5.1); the dotted lines mark the median of these curves.

For February, IDF curves from observations and BLRPM simulations exhibit large discrepancies: for all durations, the 0.99-quantile (100-yr return-level) is above the range of variability from the BLRPM and the 0.5-quantile (2-yr return level) is below for small durations. This implies, that the shape of the extreme value distribution characterised by the scale  $\sigma$  and shape parameter  $\xi$  is differs  
 230 between the two cases. This is likely due to the winter-storm Kyrill hitting Germany and Berlin on January 18<sup>th</sup> and 19<sup>th</sup> in 2007 (Fink et al., 2009). We suppose that this singular event is not sufficiently influential for BLRPM parameter estimation but does affect the extreme value analysis. For the latter only the one maximum value per month is considered. In fact, the shape parameter  $\xi$   
 235 estimated from the observational time-series shows a large value compared to the other months; in contrast, this value is estimated to be around zero from BLRPM simulations. The following section investigates this hypothesis by excluding the precipitation events due to Kyrill.



We furthermore find that the BLRPM is generally able to reproduce the observed seasonality in IDF parameters, see Fig. 6. For all parameters, the direct estimation (blue) is mostly within the range

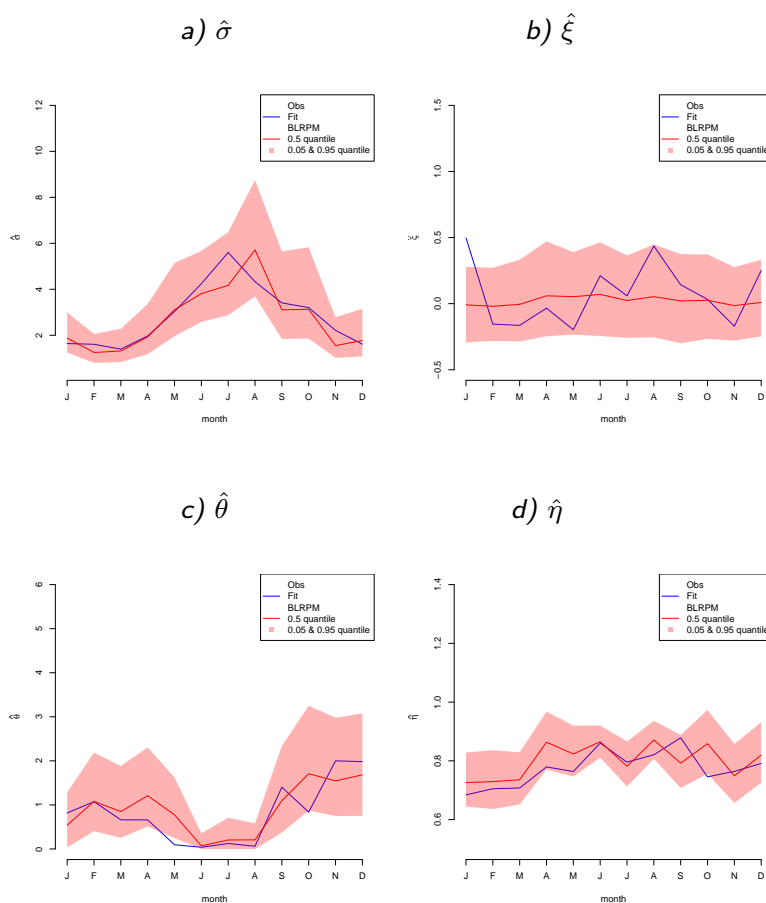


**Figure 6.** Seasonality of IDF model parameters estimated directly from the Berlin-Dahlem series (blue line), and estimated from 1000 BLRPM simulations (red). The red shadings give the range of variability (5% to 95%) from the 1000 Simulations with the median as solid red line.

240 of variability of the BLRPM simulations. For  $\hat{\sigma}$ ,  $\hat{\theta}$  and  $\hat{\eta}$ , the direct estimation (blue line) features a similar seasonal pattern as the median of the BLRPM (red line). Whereas for  $\hat{\xi}$ , the direct estimation is a lot more erratic than the median (red). As the GEV shape parameter is typically difficult to estimate Coles (2001), this erratic behaviour is not unexpected and 11 out of 12 month stay within the expected inner 90% range of variability.



### 245 5.3 Investigation of the impact of a singular extreme event

The convective cold front passage of Kyrill accounted for a maximum intensity of 24.8mm rainfall per hour, whereas the next highest value of the remaining Januaries would be 4.9mm rainfall per hour in 2002 and thus being more than 5 times lower than for Kyrill. We construct another data set without the extreme event due to Kyrill, i.e. without the year 2007. For this data set, we estimate the  
250 BLRPM parameters and simulate again 1000 time series with these new parameters. The simulated time-series were also reduced in length by one year, containing 12 years of rainfall in total. From those precipitation time series, we constructed the dd-GEV IDF curves, see Fig. 7 (right). Without

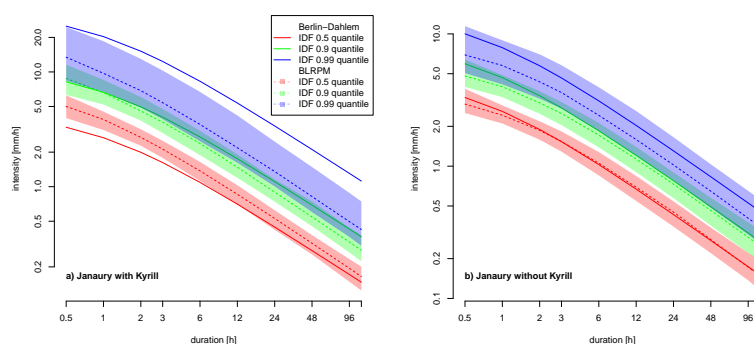


**Figure 7.** dd-GEV IDF curves for a) all Januaries (including 2007), b) Januaries excluding 2007 (different scaling on the intensity axis). Shown are the 0.5 (red), 0.9 (green) and 0.99 (blue) quantile from observations at Berlin-Dahlem (solid lines). The shaded areas are the respective 0.05 and 0.95 quantiles for the associated IDF curves obtained from 1000 BLRPM simulations.

the extreme events due to Kyrill, the BLRPM performs in January as well as in the other month with respect to reproducing the IDF relations. In particular, the spread between the 0.5-quantile (2-yr  
255 return-level) and the 0.99-quantile (100-yr) return level is reduced and the absolute values of extreme quantiles as well, cf. Fig. 7, left and right panel. Note the different scales for the intensity-axes.

### 5.4 Comparing dd-GEV IDF curves to individual duration GEV

Long time series simulated with the BLRPM can also be used to investigate adequacy of the dd-GEV model. To this end, we compare resulting IDF-curve to a GEV distribution obtained for various  
260 individual durations. The basis is a set of 1000-year simulation with the BLRPM with parameters optimised for Berlin-Dahlem. For a series of this length, we expect to obtain quite accurate (low variance) results for both, the dd-GEV IDF curve and the GEV distributions for individual durations. However, sampling uncertainty is quantified by repeatedly estimating the desired quantities from 50 repetitions. The resulting dd-GEV IDF curves are compared to the individual durations GEV in



Fig. 8 for January (left) and July (right). For most durations in January and July, the dd-IDF curves

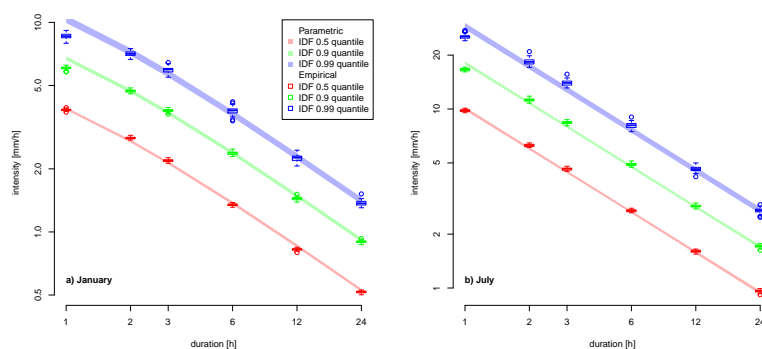


**Figure 8.** dd-GEV IDF curves for a) January and b) July and associated quantiles of a GEV distribution estimated for individual durations. Shown are the 0.5- (red), 0.9- (green) and 0.99-quantile (blue); shaded areas/box plots represent the variability over the 50 repetitions (5% to 95%)

265

are close to the quantiles of the individual duration GEV distributions. Notable differences appear for small durations and large quantiles (return-levels for long return periods); particularly in January the dd-GEV IDF model overestimates the 10-year and 100-year return-levels (duration of 1h), in July, this effect seems to be present as well but smaller in size. This is accompanied by a slight underestimation of the dd-GEV IDF for durations of 2h to 6h in July and 3h to 6h in January, most visible for the 0.99-quantile (100-yr return-level). Both effects together suggest that the flattening of the dd-GEV IDF for small durations is not sufficiently well represented. This could be due to deficiencies in the model for the duration dependent scale parameter (Eq. (4)) but might also be a consequence of an inadequate sampling of durations ( $d \in \{1h, 6h, 12h, 24h, 48h, \dots\}$ ) to be used to estimate the dd-GEV IDF parameters. This is a point for further investigation.

270

275

## 6 Discussion and conclusions

A Bartlett-Lewis rectangular pulse model (BLRPM) is optimized for the Berlin-Dahlem precipitation time series. Subsequently IDF curves are obtained directly from the original series and from simulation with the BLRPM. Basis for the IDF curves is a parametric model for the duration-dependence of the GEV scale parameter which allows a consistent estimation of one single duration-dependent GEV using all duration series simultaneously (dd-GEV IDF curve). Model parameters for the BLRPM and the IDF curves are estimated for all months of the years and seasonality in the parameters is visible. Typical small-scale convective events in summer and large-scale stratiform precipitation patterns in winter are associated with changes in model parameters.

280



285 We show that the BLRPM is able to reproduce empirical statistics used for parameter estimation;  
Mean, variance and autocovariance of simulated time-series are in good agreement with observa-  
tional values, whereas the probability of zero rainfall is more difficult to capture (cf. Rodriguez-  
Iturbe et al., 1987; Onof and Wheater, 1994a).

With respect to the first research question posed in the introduction, we investigate to what extent  
290 the BLRPM is able to reproduce the intensity-duration relationship found in observations. We show  
that they do reproduce the main features of the IDF curves estimated directly from the original time  
series. However, a tendency to underestimate return-levels associated with long return-periods is  
observed. Furthermore, IDF curves for February show a strong discrepancy between the BLRPM  
simulations and the original series. We hypothesize and investigate that this is due to the Berlin-  
295 Dahlem precipitation series containing an extreme rainfall event associated with the winter-storm  
*Kyrill* passing over Berlin during January 18<sup>th</sup> and 19<sup>th</sup>, 2007. This event is singular in the sense that  
the maximum hourly precipitation rate during these two days exceeds the second largest rate found  
in the time series by a factor of 5. This addresses the second research question: How are IDF curves  
affected by singular extreme events which might not be reproducible with the BLRPM? When the  
300 year 2007 is excluded from the analysis, the aforementioned discrepancy in January disappears. We  
conclude that such a singular extreme event has the potential to influence the dd-GEV IDF curve as  
1 out of 13 values per duration – i.e. one maximum per year out of a 13 years time series – does  
change the GEV distribution. However, its potential to influence mean and variance statistics used  
to estimate BLRPM parameters is minor.

305 The third questions addresses the validity of the duration dependent parametric model for the  
GEV scale parameter which allows a consistent estimation of IDF curves. For a set of long simu-  
lations (1000 years) with the BLRPM, the comparison of IDF curves with the duration-dependent  
GEV approach with quantiles from a GEV estimated from individual durations suggest a systematic  
discrepancy associated with the flattening of the IDF curve for short durations. Quantiles from in-  
310 dividual durations are smaller for small durations as the dd-GEV IDF curves which challenges the  
latter modeling approach. However, instead of altering the duration dependent formulation of the  
scale parameter  $\sigma_d$  (Eq. (4)), a different sampling strategy for durations  $d$  used in the estimation of  
the dd-GEV parameters might alleviate the problem. This is a topic for further investigation.

We do not find the BLRPM producing unrealistically high precipitation amounts, as discussed for  
315 the random- $\eta$  model (Verhoest et al., 2010). Nevertheless, improvements in reproducing the observed  
extreme value statistics (especially large return levels) could be made by adding the third moment in  
parameter estimation, as previous studies showed (Kaczmarek, 2011).

In summary, the BLRPM is able to reproduce the general behaviour of extremes across multiple  
time scales (durations) as represented by IDF curves. Singular extreme events do not have the poten-  
320 tial to change the BLRPM parameters but they do effect IDF statistics and consequently modifies the



previous conclusion for these cases. A duration dependent GEV is a promising approach to obtain consistent IDF curves; its behaviour at small durations needs further investigation.

### Appendix A: BLRPM parameters

Using a Latin-Hypercube approach, we generated 100 different sets of initial guesses for the parameters used in the numerical optimization of the symmetrized objective function, Eq. (2). The estimation of BLRPM parameters proved to be robust and the majority of optimisations led to the same minimum of the objective function which is then assumed to be the global minimum. Parameter estimates are given in Tab. 1.

	$\hat{\lambda}$ [h <sup>-1</sup> ]	$\hat{\gamma}$ [h <sup>-1</sup> ]	$\hat{\beta}$ [h <sup>-1</sup> ]	$\hat{\eta}$ [h <sup>-1</sup> ]	$\hat{\mu}_x$ [mm h <sup>-1</sup> ]	$Z_{\min}$
Jan	0.012	0.049	0.266	1.223	1.093	0.389
Feb	0.016	0.065	0.305	0.906	0.511	0.036
Mar	0.010	0.028	0.165	0.924	0.614	0.077
Apr	0.015	0.073	0.100	0.841	0.845	0.125
May	0.021	0.066	0.102	1.080	1.707	0.419
Jun	0.018	0.350	0.613	5.191	7.873	0.109
Jul	0.015	0.090	0.300	2.098	3.946	0.105
Aug	0.018	0.265	0.385	2.960	7.228	0.126
Sep	0.011	0.037	0.122	0.827	1.340	0.055
Oct	0.016	0.109	0.219	0.753	0.990	0.099
Nov	0.019	0.091	0.378	0.796	0.525	0.064
Dec	0.027	0.119	0.205	0.753	0.602	0.130

**Table 1.** Optimum of estimated BLRPM parameters for individual month of the year for the Berlin-Dahlem precipitation series and corresponding value of the objective function  $Z$

### Appendix B: Difference in IDF curves

Figure 9 shows the relative difference between IDF curves (dd-GEV) derived from the BLRPM and directly from the observational time series. From the four panels in Fig. 9, the discrepancies of the BLRPM can be highlighted. Apart from the large discrepancies in January discussed in Sect. 5.3, the range of variability (colored shadows in Fig. 9 include the zero difference line. However, the median over the 1000 BLRPM simulations show general tendency for the BLRPM to underestimate extremes for large return periods (0.99-quantile) by 25-50%. The best agreement is achieved for April.

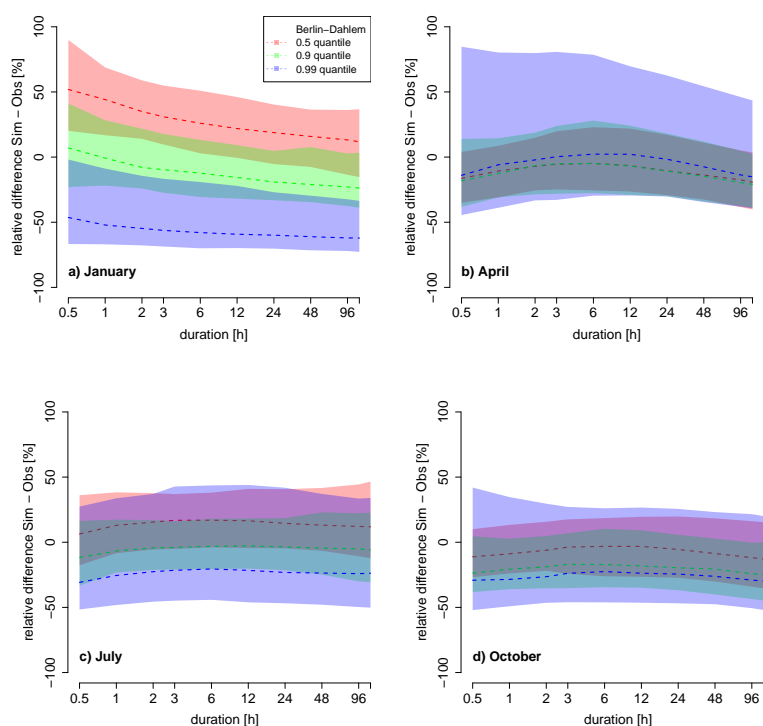


**Figure 9.** Relative differences between simulated and observed IDF curves for a) January, b) April, c) July and d) October in percent relative to the observational values. Shown are the 2-yr (0.5-quantile, red), the 10-yr (0.9-quantile, green) and 100-yr return-level (0.99- quantile, blue) differences. The dashed lines denotes the median over all 1000 simulations and the surrounding coloured shading mark the range of variability (5% to 95%). Due to the usage of transparent colours, the three different colours can overlap and mix, grey shadows thus correspond to the overlapping of all three colours.





*Acknowledgements.* The project has been funded by Deutsche Forschungsgemeinschaft (DFG) through grant CRC 1114.



## References

- 340 Austin, P. and Houze, R.: Analysis of the Structure of Precipitation Patterns in New England, *J. Appl. Meteor.*,  
11, 926–935, 1972.
- Bernard, M. M.: Formulas for rainfall intensities of long duration, *Transactions of the American Society of  
Civil Engineers*, 96, 592–606, 1932.
- Broyden, C.: The convergence of a class of double-rank minimization algorithms, *J. Instit. Math. Applications*,  
345 6, 76–90, 1970.
- Cam, L. L.: A Stochastic Description of Precipitation, *Proc. Fourth Berkeley Symp. on Math. Statist. and Prob.*,  
3, 165–186, 1961.
- Cheng, L. and AghaKouchak, A.: Nonstationary precipitation Intensity-Duration-Frequency curves for infras-  
tructure design in a changing climate., *Scientific reports*, 4, 7093–7093, 2013.
- 350 Coles, S. G.: *An Introduction to Statistical Modelling of Extreme Values*, Springer, London, 2001.
- Cowpertwait, P.: A Poisson-cluster model of rainfall: high-order moments and extreme values, *Proceedings:  
Mathematical, Physical and Engineering Sciences*, Vol. 454, No. 1971, 885–898, 1998.
- Cowpertwait, P., O’Connell, P., Metcalfe, A., and Mawdsley, J.: Stochastic point process modelling of rainfall.  
I. Single-site fitting and validation, *J. Hydrol.*, 175, 17–46, 1996a.
- 355 Cowpertwait, P., O’Connell, P., Metcalfe, A., and Mawdsley, J.: Stochastic point process modelling of rainfall.  
II. Regionalisation and disaggregation, *J. Hydrol.*, 175, 47–65, 1996b.
- Cowpertwait, P., Isham, V., and Onof, C.: Point process models of rainfall: Developments for fine-scale struc-  
ture, *Research Report 277, Departement of Statistical Science, University College London*, 2007.
- Embrechts, P., Klüppelberger, C., and Mikosch, T.: *Modelling Extremal Events for Insurance and Fincance*,  
360 Springer, Berlin, 1997.
- Fink, A. H., Brücher, T., Ermert, V., Krüger, A., and Pinto, J. G.: The European storm Kyrill in January 2007:  
synoptic evolution, meteorological impacts and some considerations with respect to climate change, *Nat.  
Haz. Earth Syst. Sci.*, 9, 405–423, 2009.
- Fletcher, R.: A New Approach to Variable Metric Algorithms, *Computer J.*, Vol. 13, No. 3, 317–322, 1970.
- 365 Goldfarb, D.: A Family of Variable Metric Updates Derived by Variational Means, *Mathematics of Computa-  
tion*, Vol. 24, No. 109, 23–26, 1970.
- Kaczmarek, J.: Further Development of Bartlett-Lewis model for fine-resolution rainfall, *Research Report 312,  
Departement of Statistical Science, University College London*, 2011.
- Khaliq, M. and Cunnane, C.: Modelling point rainfall occurrences with the Modified Bartlett-Lewis Rectangular  
Pulses Model, *J. Hydrol.*, 180, 109–138, 1996.
- 370 Kim, D., Olivera, F., Cho, H., and Scolofsky, S.: Regionalization of the Modified Bartlett-Lewis Rectangular  
Pulse Stochastic Rainfall Model, *Terr. Atmos. Ocean Sci.*, Vol.24, No. 3, 421–436, 2013.
- Koutsoyiannis, D., Kozonis, D., and Manetas, A.: A mathematical framework for studying rainfall intensity-  
duration-frequency relationships, *J. Hydrol.*, 206, 118–135, 1998.
- 375 Langousis, A. and Veneziano, D.: Intensity-duration-frequency curves from scaling representations of rainfall,  
*Water Resources Res.*, 43, n/a–n/a, w02422, 2007.
- McKay, M. D., Beckman, R. J., and Conover, W. J.: A Comparison of Three Methods for Selecting Values of  
Input Variables in the Analysis of Output from a Computer Code, *Technometrics*, 21, 239–245, 1979.



- Merz, B., Elmer, F., Kunz, M., Mühr, B., Schröter, K., and Uhlemann-Elmer, S.: The extreme flood in June  
380 2013 in Germany, *La Houille Blanche*, pp. 5–10, 2014.
- Nelder, J. and Mead, R.: A Simplex Method for Function Minimization, *Computer J.*, 7 (4), 308–313, 1965.
- Neyman, J. and Scott, E.: A theory of the spatial distribution of galaxies., *Astrophys. J.*, 116, 144, 1952.
- Onof, C. and Wheater, H.: Improved fitting of the Bartlett-Lewis Rectangular Pulse Model for hourly rainfall,  
*Hydrological Sciences*, Vol. 39, No. 6, 663–680, 1994a.
- 385 Onof, C. and Wheater, H.: Improvements to the modelling of British rainfall using a modified Random Param-  
eter Bartlett-Lewis Rectangular Pulse Model, *J. Hydrol.*, 157, 177–195, 1994b.
- Onof, C., Chandler, R., Kakou, A., Northrop, P., Wheater, H., and Isham, V.: Rainfall modelling using Poisson-  
cluster processes: a review of developments, *Stochastic Environmental Research and Risk Assessment*, 14,  
184–411, 2000.
- 390 Pattison, A.: Synthesis of hourly rainfall data, *Water Resour. Res.*, 1 (4), 489–498, 1956.
- R Core Team: R: A Language and Environment for Statistical Computing, R Foundation for Statistical Com-  
puting, Vienna, Austria, <https://www.R-project.org/>, 2016.
- Rodriguez-Iturbe, I., Cox, D., F.R.S., and Isham, V.: Some models for rainfall based on stochastic point pro-  
cesses, *Proc. R. Soc. Lond., A* 410, 269–288, 1987.
- 395 Rodriguez-Iturbe, I., Cox, D., and Isham, V.: A point process model for rainfall: further developments, *Proc. R.*  
*Soc. Lond., A* 417, 283–298, 1988.
- Shanno, D.: Conditioning of quasi-Newton methods for function minimization, *Mathematics of Computation*,  
Vol. 24, No. 111, 647–656, 1970.
- Simonovic, S. P. and Peck, A.: Updated rainfall intensity duration frequency curves for the City of London  
400 under the changing climate, Department of Civil and Environmental Engineering, The University of Western  
Ontario, 2009.
- Smithers, J., Pegram, G., and Schulze, R.: Design rainfall estimation in South Africa using Bartlett-Lewis  
rectangular pulse rainfall models, *J. Hydrol.*, 258, 83–99, 2002.
- Soltyk, S., Leonard, M., Phatak, A., Lehmann, E., et al.: Statistical modelling of rainfall intensity-frequency-  
405 duration curves using regional frequency analysis and bayesian hierarchical modelling, in: *Hydrology and*  
*Water Resources Symposium 2014*, p. 302, Engineers Australia, 2014.
- Vandenbergh, S., Verhoest, N., Onof, C., and De Baets, B.: A comparative copula-based bivariate frequency  
analysis of observed and simulated storm events: A case study on Bartlett-Lewis modeled rainfall, *Water*  
*Resources Research*, 47, 2011.
- 410 Vanhaute, W., Vandenbergh, S., Scheerlinck, K., De Baets, B., and Verhoest, N.: Calibration of the modified  
Bartlett-Lewis model using global optimization techniques and alternative objective functions, *Hydrology*  
*and Earth System Sciences*, 16, 873–891, 2012.
- Verhoest, N., Troch, P., and Troch, F. D.: On the applicability of Bartlett-Lewis Rectangular pulse models in the  
modeling of desing storms at a point, *J. Hydrol.*, 202, 108–120, 1997.
- 415 Verhoest, N. E., Vandenbergh, S., Cabus, P., Onof, C., Meca-Figueras, T., and Jameleddine, S.: Are stochastic  
point rainfall models able to preserve extreme flood statistics?, *Hydrological processes*, 24, 3439–3445, 2010.
- Waymire, E., Gupta, V., and Rodriguez-Iturbe, I.: A spectral theory of raifnall intensity at the meso- $\beta$  scale,  
*Water Resour. Res.*, 20(10), 1453–1465, 1984.



420 Wheeler, H., Chandler, R., Onof, C., Isham, V., Bellone, E., Yang, C., Lekkas, D., Lourmas, G., and Segond,  
M.-L.: Spatial-temporal rainfall model for flood risk estimation, *Stoch. Environ. Res. Risk. Assess.*, 19,  
403–416, 2005.